JOURNAL OF VIROLOGY, Oct. 1997, p. 7648–7656 Vol. 71, No. 10
0022-538X/97/$04.00+0


# Multiple Biological Roles Associated with the Rous Sarcoma Virus 5′ Untranslated RNA U5-IR Stem and Loop

JENNIFER T. MILLER, ZHENG GE, SHANNON MORRIS, KINGSHUK DAS, AND JONATHAN LEIS*

*Department of Biochemistry, Case Western Reserve University School of Medicine, Cleveland, Ohio 44106-4935*

Received 8 May 1997/Accepted 15 July 1997

**The 5′ untranslated region of Rous sarcoma virus (RSV) RNA is a highly ordered structure involved in multiple processes in the viral replication cycle. One of these structures, referred to as the U5-IR stem, is located immediately upstream of the 5′ end of the primer binding site. Disruption of its base pairing results in a decrease in initiation of reverse transcription (D. Cobrinik, A. Aiyar, Z. Ge, M. Katzman, H. Huang, and J. Leis, J. Virol. 65:3864–3872, 1991). In the present study, the length of the U5-IR stem structure has been extended by insertions of different sequences which decrease the efficiency of reverse transcription, in vivo and in vitro. Reverse transcription is rescued partially by placing single-stranded bulges into the middle of the extended duplexes. Nucleotide substitutions or insertions into the loop region of the U5-IR stem also decrease the efficiency of reverse transcription, suggesting that these sequences may specifically interact with reverse transcriptase. Surprisingly, all of the extended stem mutations cause significant RNA packaging defects. In contrast, nucleotide insertions or base substitutions in the U5-IR loop do not affect RNA packaging. These data indicate that the reverse transcription initiation complex and RNA packaging apparatus are influenced by the same region of RSV RNA and that each process is differentially sensitive to changes in sequence and/or secondary structure.**

The 5′ noncoding region of retroviral genomic RNA is predicted to fold into a series of RNA secondary structures which regulates the process of reverse transcription (8, 9, 13, 17, 29, 37). In avian retroviruses, these structures are located near the primer binding site (PBS) and include the U5-leader stem and the U5-IR stem (see Fig. 1A). The U5-leader stem is formed by sequences within U5 and the leader. Mutations that disrupt the structure impair initiation of reverse transcription in infected cells, whereas mutations that alter the sequence but retain the structure have no effect (13). The U5-IR stem is composed of an inverted repeat in U5 adjacent to the PBS. Perturbation of this structure affects initiation of reverse transcription in a manner similar to that seen with disruptions of the U5-leader stem (12). Both the U5-leader and U5-IR stem structures have been detected by nuclease mapping (35a). In addition to these structural elements, there are at least two regions of the viral RNA which are predicted to interact directly with the $tRNA^{Trp}$ primer. One is the PBS, which is complementary to the 3′ end of $tRNA^{Trp}$. The other is the U5 RNA sequence located between the U5-IR and U5-leader stems, which is complementary to the TψC arm of $tRNA^{Trp}$ (12, 14).

Other retroviruses are predicted to form similar, but not identical, U5 RNA secondary structures (8, 9, 37, 41). For a review of these structures, see Leis et al. (29). In the case of Moloney murine leukemia virus (Mo-MuLV), deletions in the corresponding U5-IR stem result in defective initiation of cDNA synthesis (39). In human immunodeficiency virus type 1 (HIV-1), regions of 5′ noncoding RNA, in addition to the PBS, are proposed to interact with the $tRNA_3^{Lys}$ primer. One such region is the single-stranded loop formed by the U5-IR stem, which can base pair with the anticodon loop of $tRNA_3^{Lys}$. Disruption of this interaction adversely influences initiation of reverse transcription (6, 7, 20, 46, 47). In addition, replication of proviral constructs containing an altered PBS is stabilized by alteration of the U5-IR loop sequences to those complementary to the new primer tRNA anticodon loop (22, 23, 50). Thus, the U5-IR loop sequence of HIV-1 is probably analogous to the avian U5-TψC interaction region. HIV-1 RNA sequences downstream of the PBS are also reported to interact with the tRNA primer (27, 31), although the significance of this interaction is not clear. In the present study, we show that extension of the potential base pairing in the U5-IR stem as well as changes in loop sequence causes reverse transcription defects. In addition, several of the stem mutations caused a significant decrease in the amount of RNA encapsidated into particles. Thus, the integrity of the U5 region near the PBS is required for multiple biological functions in viral replication.

## MATERIALS AND METHODS

**Reagents.** *Escherichia coli* DNA polymerase I, Klenow fragment (5 U/μl), restriction enzymes, proteinase K (15 mg/ml), and deoxynucleoside and ribonucleoside triphosphates were purchased from Boehringer Mannheim Biochemicals. RNase A (1 mg/ml) was from 5′→3′. T4 polynucleotide kinase (10 U/μl) and T4 DNA ligase (400 U/μl) were purchased from New England Biolabs. T7 RNA polymerase (20 U/μl), RNasin, RNase inhibitor (40 U/μl), and RQ1 DNase (1 U/μl) were purchased from Promega. Avian myeloblastosis virus (AMV) reverse transcriptase (RT) (30 U/μl) was obtained from Molecular Genetics Resources. The sequencing kit, Sequenase v2.0, was obtained from United States Biochemicals. All enzymes were used according to the manufacturer's specifications. [α-$^{32}$P]dCTP (3,000 Ci/mmol) and [γ-$^{32}$P]ATP (6,000 Ci/mmol) were obtained from New England Nuclear. Oligodeoxynucleotides were synthesized on an Applied Biosystems 380B nucleic acid synthesizer and purified as previously described (3). pGEM3z DNA was purchased from Promega. Other chemicals were of the highest grade available and were purchased from either Sigma Biochemicals or Fisher Chemicals.

**Bacterial strains and plasmid purification.** All vectors were transformed into *E. coli* DH5α (obtained from Stratagene). Detailed maps of, and growth conditions for, pDC101B and pDC102B were as previously described (13). Plasmids were isolated by the alkaline lysis procedure and purified by equilibrium cesium chloride density gradient centrifugation (42). The pDC101S vector was derived

* Corresponding author. Mailing address: Department of Biochemistry, Case Western Reserve University, 2119 Abington Rd., Cleveland, OH 44106-4935. Phone: (216) 368-3360. Fax: (216) 368-4544. E-mail: jx18@biocserver.bioc.cwru.edu.

from pDC101B (12) by the insertion of a single base change from T57 to C57, which introduced a *Sal*I site into the vector (43). The growth behavior of virus derived from pDC101S is indistinguishable from that of pDC101B-derived virus.

**Computer analysis of the U5-IR structures.** The program and parameters used to analyze RNA secondary structures were as described elsewhere (13). The free energy of the structure depicted in Fig. 1A is −40.8 kcal/mol.

**Mutagenesis of the U5-IR stem-loop.** Substitutions of 3 (S3L) or 5 (S5L) nucleotides or insertion of 4 nucleotides (I4L) into the U5-IR loop were constructed by overlap mutagenesis PCR (3) using primers A and B and mutagenic primers S3L, S5L, and I4L, respectively. The sequences of the oligodeoxynucleotides are listed below. A first round of PCR was carried out with pDC101S as the wild-type template amplified with primer B and the respective mutagenic primer. The product of this amplification was purified by 1% agarose gel electrophoresis containing 1× TBE (89 mM Tris, 89 mM boric acid, and 2 mM EDTA) and ethidium bromide. DNA bands were visualized by UV light and were isolated from the gel by electrophoresis-driven transfer onto DE-81 filter paper from Whatman. The product DNA was recovered from the filters by elution with 50 mM Tris-HCl (pH 8.0)–1 M NaCl–10 mM EDTA followed by precipitation with 2 volumes of ethanol. A second round of PCR was carried out with the product from the first round and pDC101S DNA, at a molar ratio of 5 to 1, as templates. Primers A and B were used to amplify the final product in the second round of PCR.

A one-round PCR protocol using the I12L/S mutagenic primer, primer B, and pDC101S as the template introduced the I12L/S mutation. PCR conditions were the same as above. The mutations DS, RDS, B3DS, B3RDS, I12Lpk, and I12Lss (described in Results and depicted in Fig. 1B) were introduced into pDC101S by two rounds of PCR. In the first round, primer A and mutagenic primer (minus strand) were used to amplify pDC101S. In a concomitant but separate reaction, primer B and mutagenic primer (plus strand) were used to amplify pDC101S. The two products were purified as described above and used as templates, in equimolar amounts, in a second round of PCR which employed only primers A and B.

The list of oligodeoxynucleotides used for PCR mutagenesis is as follows: I4L, 5′AATGAAGCAG**TCTC**AAGGCTTCATTTG3′; S3L, 5′AATGAAGC**GCT**AGGCTTCATTTG3′; S5L, 5′AATGAAGC**GCTT**CGCTTCATTTG3′; I12L/S, 5′TGGCCGGACCGTCGACTCCCTAACGATTGCGAACACCTGAATGAAGC**CTTCTCTCTTCG**AGAAGGCTTCATTTG3′; DS(+), 5′**TGAAGC**AGAAGG**CTTCA**GCTTCATTTGGTGACCCC3′; DS(−), 5′**TGAAGC**CTTCT**GCTTCA**GCTTCATTCAGGTGTTCGC3′; RDS(+), 5′**CTTCTC**AGAAG**GAGAAG**GCTTCATTTGGTGACCCC3′; RDS(−), 5′**CTTCTC**CTTCT**GAGAAG**GCTTCATTCAGGTGTTCGC3′; B3DS(+), 5′**CTGTGAAGC**AGAAG**GCTTCAGTC**GCTTCATTTGGTGACCCC3′; B3DS(−), 5′**GACTGAAGC**CTTCT**GCTTCACAG**GCTTCATTCAGGTGTTCGC3′; B3RDS(+), 5′GAAGC**CTGCTTCTC**AGAAG**GAGAAGGTC**GCTTCATTTGGTGACCCC3′; B3RDS(−), 5′GAAGC**GACCTTCTC**CTTCT**GAGAAGCAG**GCTTCATTCAGGTGTTCGC3′; I12Lpk(+), 5′**GAGAGGGAAGGG**AGAAGGCTTCATTTGGTGACCCC3′; I12Lpk(−), 5′CTTCT**CCCTTCCCTCTC**GCTTCATTCAGGTGTTCGC3′; I12Lss(+), 5′GAAGC**GAAAGAAAGAAA**AGAAGGCTTCATTTGGTGACCCC3′; I12Lss(−), 5′GAAGCCTTCT**TTTCTTTCTTTC**GCTTCATTCAGGTGTTCGC3′; Primer A(+), 5′GCCATTTTACCATTC3′; and Primer B(−), 5′GGGAAGGATACAAAGGACTC3′. The bold letters indicate changes introduced for each mutation; the plus and minus signs refer to the respective DNA strand primers; the underlined sequence in the I12L/S oligodeoxynucleotide is a *Sal*1 site.

All PCR-amplified DNAs were cloned into the vector pDC101S after digestion of both with *Sal*I and *Sac*I according to the manufacturer's recommendations. Sequencing identified positive clones. The percentage of positive clones was greater than 80% under these conditions. The modified pDC101S DNAs were then digested with *Eco*RV and ligated to *Eco*RV-digested pDC102B for introduction into QT6 cells (12).

**Transfection and virus assays.** Mutant DNAs were introduced into QT6 cells and stably transfected cell lines were established by selection with G418 as previously described (12). Viral growth was monitored by assaying RT activity from viral particles released into the cell media by using exogenous template and primer (12).

**Analysis of reverse transcription in virus particles with endogenous primer and template.** Media from one or two successive 12-h incubations were collected from wild-type or mutant cell lines cultured on 150-mm tissue culture dishes and spun for 10 min at 4,000 × *g* at room temperature to remove cellular debris. Virus was then collected by centrifugation of the clarified supernatants through a 5-ml cushion of 20% sucrose in 50 mM Tris-HCl (pH 8.0)–1 mM EDTA (5TE) at 85,000 × *g* for 100 min at 4°C in a Beckman SW28 rotor. The media and sucrose cushion were removed, and the tubes were drained by inversion at 4°C for 5 min. Residual liquid was aspirated. Pelleted virus was suspended in 5TE buffer, and the amount of particles present was determined by analyzing serial dilutions for RT activity by using saturating levels of poly(G) and oligo(dC)$_{12–18}$ as exogenous template and primer, respectively.

To examine endogenous reverse transcription, all samples were normalized to the amount of virus that incorporates 0.1 pmol of dCMP in 30 min in the exogenous template-primer RT assay. Equivalent quantities of particles were incubated for 10 min at 37°C in a volume of 26 μl containing 100 mM Tris-HCl (pH 8.0), 25 mM NaCl, 3 mM $MgCl_2$, 3 mM dithioerythreitol, and 12.5 μg of mellitin (Sigma)/ml. Subsequently, a deoxynucleotide cocktail was added to a final volume of 30 μl, resulting in concentrations of 1 mM (each) dATP, dTTP, and dGTP, and 0.1 mM [α-$^{32}$P]dCTP (3,000 Ci/mmol). Reaction mixtures were incubated for 30 min at 37°C, and the reaction was stopped by the addition of 5 volumes of 5TE with 1% sodium dodecyl sulfate and a 5′-$^{32}$P-end-labeled DNA fragment of 57 bases as a recovery standard. This mixture was extracted with phenol-chloroform and chloroform, followed by precipitation of the DNA with ethanol. Strong-stop DNA was collected by centrifugation, and the pellets were suspended in 0.25 mM NaOH followed by incubation at 65°C for 15 min. At that time, samples were neutralized and again precipitated with ethanol. DNA products were analyzed by denaturing polyacrylamide gel (6% acrylamide, 0.4% bisacrylamide, 7 M urea) electrophoresis in the presence of TBE buffer. Products were visualized by autoradiography. Bands on the films were quantified with a Hewlett-Packard Scan Jet and the computer software program NIH Image.

For examination of initiation of reverse transcription in mellitin-activated virions, the above conditions were used with the exceptions that only [α-$^{32}$P] dATP was added to the reaction, a 5′-$^{32}$P-end-labeled DNA fragment of 95 bases was added as a recovery standard, and products were analyzed by denaturing gel electrophoresis without prior digestion with alkali.

**Preparation of viral RNAs in vitro.** RNA templates of 270 nucleotides starting from the first base in R were prepared with T7 RNA polymerase as previously described (35). Briefly, a PCR fragment of DNA was prepared by using a 5′ primer containing the promoter for T7 RNA polymerase and template DNA, pDC101S, carrying various mutations as indicated. This PCR product was used as a transcription template to create a T7 RNA polymerase runoff product in a 100-μl reaction mixture containing 40 mM Tris-HCl (pH 7.9), 6 mM $MgCl_2$, 2 mM spermidine, 15 mM dithiothreitol, 1 mM (each) ATP, UTP, CTP, and GTP, 2 μg of template DNA, and 125 U of T7 RNA polymerase. RNAs were then treated with 1 U of RQ1 DNase at 37°C for 30 min, extracted once with phenol and three times with chloroform, and purified by 2% agarose–TBE gel electrophoresis. RNA was recovered as described in the previous section for the PCR products, except that all reagents were RNase free. RNAs were precipitated by the addition of 3 volumes of ethanol, collected by centrifugation, and suspended in water, and concentrations were determined by UV absorbance at 260 nm. The 28-mer primer RNA, used to reconstitute reverse transcription in vitro, was prepared as described previously (1).

**Reconstitution of reverse transcription in vitro.** In vitro reverse transcription reactions were performed as described previously (2). Briefly, RNA transcripts (270 nucleotides) bearing either wild-type or mutant sequences (as indicated) were incubated with a 28-nucleotide RNA primer representing the 3′ end of tRNA$^{Trp}$ and with AMV RT in a 30-μl reaction volume containing 50 mM Tris-HCl (pH 8.0), 100 mM KCl, 5 mM $MgCl_2$, 3 mM dithioerythreitol, 1 mM (each) dATP, dGTP, and dTTP, and [α-$^{32}$P]dCTP (0.1 mM; 6.7 Ci/mmol). One picomole of a DNA primer was also added as an internal control of input RNA. This primer anneals to the 5′ U5 sequence of the template and produces a runoff DNA product of 40 deoxynucleotides. After incubation at 37°C for 40 min, the reaction mixture was extracted with phenol-chloroform and the DNA was precipitated as described above. The DNA was pelleted by centrifugation and suspended in 0.25 M NaOH. After incubation at 65°C for 15 min, the mixture was neutralized with 0.1 volume of 0.3 M sodium acetate, pH 5.2, and the DNA was again precipitated with ethanol. The DNA was pelleted, suspended, and loaded onto 6% acrylamide gels containing 7 M urea. After electrophoresis, products were visualized by autoradiography. Bands were quantified as described above.

**Quantitation of viral RNA content in virus particles.** Virus particles were collected from tissue culture cell supernatants by centrifugation through a 20% sucrose cushion as described above. The amount of virus was quantified by RT activity and immunoblotting with an antibody directed against the viral capsid protein. The RT assay was carried out as previously described (13). Immunoblotting was performed after spotting serial dilutions of virus particles onto nitrocellulose membranes by using a dot blot apparatus. The membrane was then blocked overnight with 3% nonfat dry milk solubilized in TBS (16 mM Tris-HCl [pH 7.6]–400 mM NaCl). After washing with TBS, a rabbit-derived polyclonal antibody directed against AMV capsid was applied and the membrane was placed on a rocker for 2 h. The membrane was washed again, and a secondary antibody (goat antirabbit antibody conjugated with horseradish peroxidase) was added. After 1 h of shaking, peroxidase substrate was added and signals were visualized and quantitated by chemiluminescence. All results reported in this article fall in the linear range of the RT and the immunoblotting assay.

A primer extension assay was used to quantify genomic RNA extracted from virus particles. Equal amounts of virus particles (capable of incorporation of 0.1 pmol of dCMP by using an exogenous template-primer assay) were treated with 60 μg of proteinase K/ml and 0.2% sodium dodecyl sulfate for 60 min at 37°C and then extracted with phenol-chloroform as described above. RNAs were precipitated with ethanol in the presence of 0.3 M sodium acetate and 5 μg of glycogen. For measurement of the amount of genomic RNA, a primer that annealed to the U5 sequence from nucleotide 40 to 20 was used. Prior to use, the primer was 5′ end labeled, separated by gel electrophoresis, eluted from the gel, and purified by using a $C_{18}$ reverse-phase column. The purified primer was then incubated with virus-derived RNA in boiling water for 30 s, followed by incubation at 40°C for 1 min. The annealing mixture was brought to 22 mM KCl–22 mM Tris-HCl (pH 8.0) and incubated at 40°C for another 10 min. Five units of AMV RT, deoxynucleoside triphosphates (0.55 mM [each] dATP, dTTP, dGTP, and dCTP), 6 mM $MgCl_2$, and 6 mM dithioerythritol were added, and the mixture

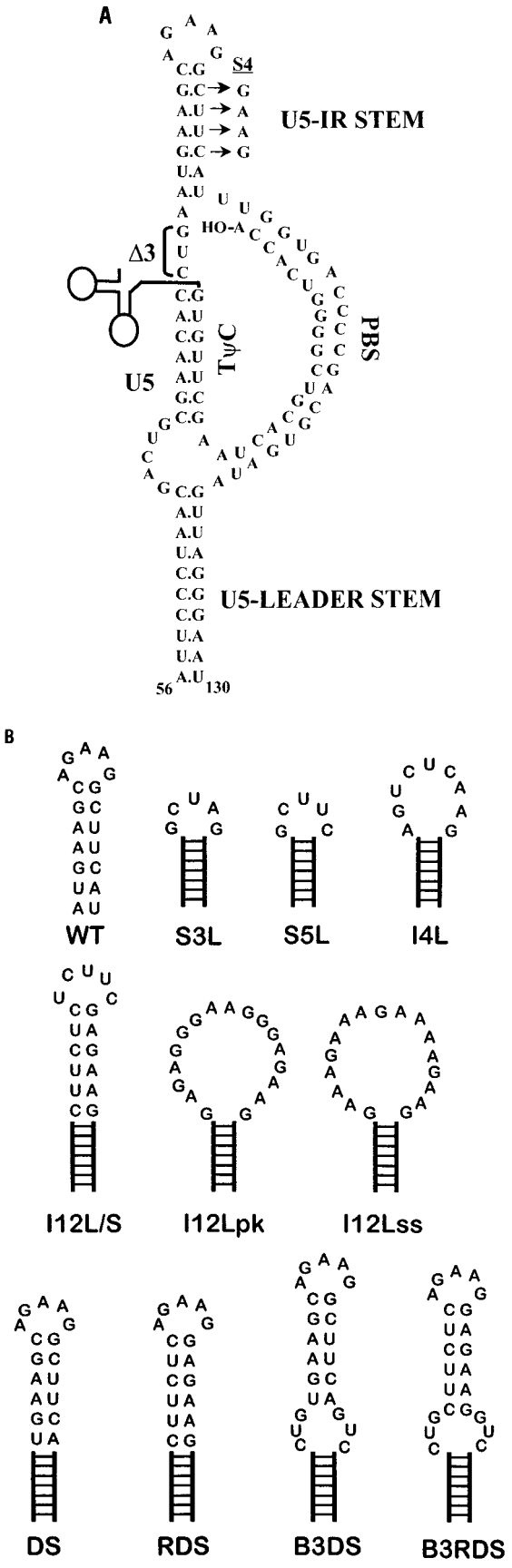


FIG. 1. (A) Predicted secondary structure for the 5′ noncoding region of avian sarcoma virus (Schmidt Ruppin A) RNA near the PBS. The numbers indicate nucleotides from the viral RNA 5′ end. U5 denotes nucleotide sequences located between the 5′ end of the viral RNA and the PBS; PBS denotes the minus-strand primer binding site. The U5-IR and U5-leader stems and the U5-TψC interaction region are as indicated. The base substitutions in the U5-IR stem associated with the S4 mutation (12) are indicated by the arrows. The Δ3 mutation (2) is defined by the bracket. (B) Schematic representation of the U5-IR stem and loop regions of wild-type and mutant constructs. The sequence of the wild-type Schmidt Ruppin A avian sarcoma virus stem and loop region is diagrammed at the top left (WT). In mutant constructs, the wild-type stem sequence is represented by the "ladder" structure. The sequences that have been changed or inserted and the structures that are predicted are shown for each specific mutant.

was incubated at 37°C for 30 min. The reaction was stopped by extraction with phenol-chloroform, and the products were ethanol precipitated after a 57-mer $^{32}$P-5′-end-labeled DNA was added as an internal control of recovery. Reaction products were loaded onto a denaturing 10% acrylamide gel for electrophoresis. The amount of primer extension DNA products was evaluated with a Hewlett-Packard Scan Jet and the computer software program NIH Image. The conditions used in this assay fell within the linear response range.

**Quantitation of viral RNA in transfected cells.** Cells from two 150-mm plates were treated with GTC [4 M guanidinium thiocyanate, 0.5% sodium-*N*-lauroyl sarcosinate, 20 mM $Na_2EDTA$, 50 mM piperazine-*N*,*N*′-bis(2-ethanesulfonic acid) (PIPES), and 0.2 M β-mercaptoethanol] and immediately homogenized for 30 s. Samples were then layered onto a cushion of 5.7 M CsCl and subjected to centrifugation at 25,000 rpm for 16 h at 22°C in a Beckman SW40 rotor. The pellet was suspended with 5TE, and the optical density at 260 nm was determined. Primer extension of 10 μg of total cellular RNA was carried out by the procedure described above.

## RESULTS

**Construction of U5-IR stem and loop mutations.** The sequence of avian sarcoma virus, Schmidt Ruppin A strain, from nucleotide 56 to 130 is depicted in Fig. 1A. The $tRNA^{Trp}$ primer is shown bound to both the PBS and the U5-TψC interaction region. The U5-IR and U5-leader stem structures are also shown. A series of mutations (Fig. 1B) were introduced into the U5-IR stem and loop as described in Materials and Methods. Mutations that alter the U5-IR loop sequence are referred to as S3L, S5L, I4L, or I12L/S, I12Lpk, and I12Lss, and represent base substitutions of 3 and 5 nucleotides or insertions of 4 or 12 nucleotides, respectively. The nomenclature used for each mutant refers to the type and position of the mutation. For instance, S3L represents a substitution of 3 nucleotides into the U5-IR loop. The I12L/S insertion contains an inverted repeat sequence predicted to extend the potential length of the U5-IR stem as well as to change the loop sequence. The I12Lpk insertion enlarges the loop by 12 nucleotides. While it does not contain an inverted repeat sequence, as does I12L/S, nucleotides in the I12Lpk loop can anneal to either UUCCCU in U5 or CCCUC in the leader to potentially form a tertiary pseudoknot structure. The I12Lss mutation also inserts 12 nucleotides into the loop. In contrast to I12Lpk and I12L/S, I12Lss neither has an internal inverted repeat sequence nor is able to form stable duplexes with the template RNA used in these studies. Thus, the 12-nucleotide insertion, I12Lss, is predicted to remain single stranded.

Mutations which alter only the U5-IR stem include DS, RDS, B3DS, and B3RDS. The DS mutation duplicates 6 bp of the U5-IR stem, while the RDS mutation introduces 6 bp of random sequence into the stem. Both of these mutants maintain a wild-type U5-IR loop. The B3DS and B3RDS mutations introduce a 3-nucleotide noncomplementary bulge into the extended U5-IR DS and RDS stem structures, respectively. The S4 mutation, as shown in Fig. 1A, disrupts the U5-IR stem (13). Also shown is the Δ3 mutation, described previously (2).

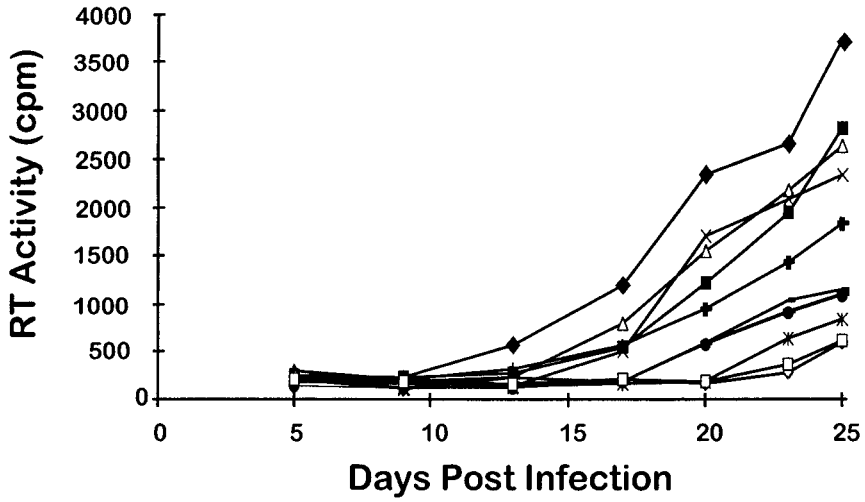


FIG. 2. Mutations in the U5-IR stem and loop cause a delay in viral growth. Equivalent amounts of wild-type and U5-IR mutant viruses were used to infect QT6 cells, and the appearance of progeny virus in the culture supernatants was determined by an RT assay at the indicated days after infection. The data represent the averages of three independent infection experiments. Symbols: ◆, wild type; ■, S3L; △, S5L; ×, I4L; ✚, I12Lss; ▬, DS; ▭, RDS; ●, I12Lpk; ✳, I12L/S; □, B3RDS; ◇, B3DS.

**Effect of U5-IR mutations on viral growth.** Viruses containing each of the above mutations were harvested from quail cell producer lines as described in Materials and Methods. Equivalent amounts of each virus, determined by RT assay, were used to infect quail fibroblasts, and the release of progeny virus into the cell media was monitored by using the RT assay as described previously (13). The growth data is presented in Fig. 2. All of the mutations resulted in viruses with various degrees of delayed growth relative to the wild type. Viruses containing loop substitutions (S3L or S5L) or loop insertions (I4L or I12Lss) grew slightly more slowly than the wild type (Fig. 2). Viruses with extended stem mutations (DS, RDS, B3DS, B3RDS, or I12L/S) exhibited a more pronounced delayed-growth phenotype (Fig. 2). The delayed appearance of virus, in each case, was not caused by a reversion event. Viruses containing each mutation, collected 20 to 25 days after the initial infection, grew with the same delayed properties when introduced into fresh cells (data not shown).

**Analysis of reverse transcription initiation and elongation in permeabilized virions.** To understand why these viruses grew slowly, mellitin-activated virions were examined for their ability to initiate reverse transcription with the endogenous genomic RNA and $tRNA^{Trp}$ primer. In this system, cDNA synthesis is initiated from the 3′-OH end of the $tRNA^{Trp}$ primer complexed to viral RNA, such that the first two deoxynucleotides incorporated are $^{32}P$-labeled dAMP residues (Fig. 3B). Therefore, the amount of $tRNA^{Trp}$-$dAMP_2$ product detected is a measure of the efficiency of initiation of reverse transcription. The $tRNA^{Trp}$-$dAMP_2$ product, after recovery from virus, migrates on an acrylamide gel as a band corresponding to 78-mer RNA. As shown in Fig. 3A, the amount of $tRNA^{Trp}$-$dAMP_2$ product detected from equivalent amounts of virions containing each of the above mutations was less than that from the wild type. The least amount of $tRNA^{Trp}$-$dAMP_2$ was found in virions containing the predicted extended-stem structures, I12L/S, DS, RDS, B3DS, and B3RDS. These are the same viruses which exhibited the most pronounced reductions in growth. In each case, the relative amount of $tRNA^{Trp}$-$dAMP_2$ product recovered from these viruses, compared to that from the wild type, was less than or approximately equal to that recovered from a previously described virus containing the U5-IR stem disruption mutation, S4 (Fig. 3A, lane 9). In contrast to the extended-stem mutant viruses, almost wild-type levels of product were obtained with the S5L and I12Lss U5-IR loop mutants. Less product was observed with the I4L or I12Lpk loop insertion mutations. As a control, no product was detected in the media of mock-infected cells.

The differences in the amount of $tRNA^{Trp}$-$dAMP_2$ product observed in Fig. 3A are not related to differences in the level of RT present in the mutant viruses. This conclusion is based on the finding that equal amounts of the mutant viruses, as

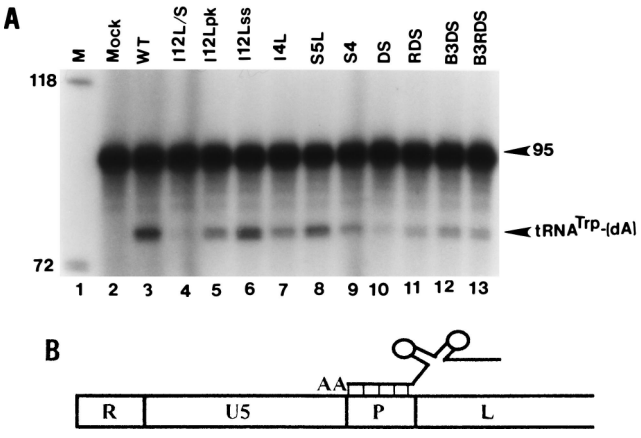


FIG. 3. Analysis of initiation of reverse transcription in mellitin-activated virions obtained from wild-type and U5-IR mutant cell lines. (A) Amounts of $tRNA^{Trp}$ primer extension products formed after a 30-min incubation of virions with mellitin and [$\alpha$-$^{32}P$]dATP as described in Materials and Methods. The migration positions of the $tRNA^{Trp}$-$[dA]_2$ product and a 5′-$^{32}P$-end-labeled DNA fragment of 95 bases, added as a recovery standard, are as indicated. Lane 1, marker DNAs of 72 and 118 deoxynucleotides. Viral products from the media of mock-infected (lane 2) or wild-type virus-infected (WT; lane 3) cells are as indicated. Products from virions containing the U5-IR mutants I12L/S (lane 4), I12Lpk (lane 5), I12Lss (lane 6), I4L (lane 7), S5L (lane 8), S4 (lane 9), DS (lane 10), RDS (lane 11), B3DS (lane 12), and B3RDS (lane 13) are as indicated. Mutations are defined in Results and depicted in Fig. 1B. (B) Schematic representation of $tRNA^{Trp}$ hybridized to the PBS and extended by 2 dAMP residues. The RNA template is represented by the unfilled box. R, repeat region; U5, unique 5′ RNA; P, PBS; L, leader RNA.

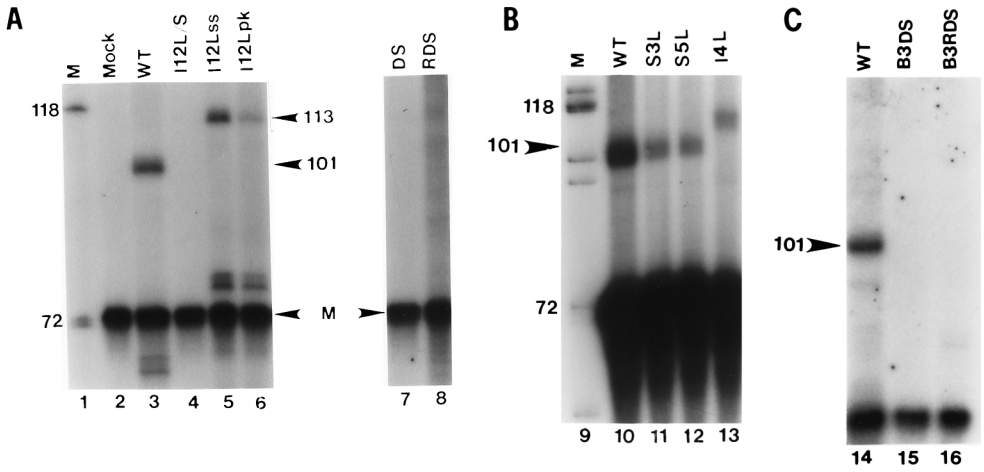


FIG. 4. Synthesis of minus-strand strong-stop cDNA in mellitin-activated virions obtained from wild-type (WT) and U5-IR mutant cell lines. (A) Amounts of strong-stop cDNA products formed with wild-type virions and with U5-IR mutants I12L/S, I12Lss, I12Lpk, DS, and RDS after a 30-min incubation of virions with mellitin, [$\alpha$-$^{32}$P]dATP, and unlabeled dTTP, dCTP, and dGTP as described in Materials and Methods. The wild-type and mutant products are labeled above their respective lanes. M between arrowheads denotes a 5′-$^{32}$P-labeled 72-base DNA fragment added to each reaction mixture upon termination to control for recovery. The migration positions of cDNA products of 101 and 113 deoxynucleotides are as shown. (B) The amounts of strong-stop cDNA products formed with wild-type virions and U5-IR mutants S3L, S5L, and I4L were analyzed as in panel A. (C) The amounts of strong-stop cDNA products formed with wild-type and U5-IR mutants B3DS and B3RDS were analyzed as in panel A.

determined by quantitation of capsid via Western blot analysis, yielded equivalent levels of DNA synthesis, as determined by an RT assay with exogenous template and primer (data not shown). Also, the differences are not related to inefficient packaging of the $tRNA^{Trp}$ primer in the mutant particles. Total RNA was isolated from equivalent amounts of wild-type and mutant virus particles and annealed to an excess of 5′-$^{32}$P-labeled primer complementary to the 3′ end of $tRNA^{Trp}$. Quantitation of a 76-deoxynucleotide RT extension product indicated that particles from all of the viruses contain equal amounts of $tRNA^{Trp}$ (data not shown).

Both initiation and elongation of reverse transcription can be analyzed in mellitin-activated virions by measuring the synthesis of strong-stop cDNA where all 4 deoxynucleotides are included during the reaction. With wild-type virus, strong-stop cDNA is 101 deoxynucleotides ($cDNA_{101}$). This represents the distance from the 3′-OH end of the tRNA primer to the 5′ end of the template RNA (Fig. 4A, lane 3). In contrast to the products analyzed in Fig. 3A, the cDNAs are treated with alkali to remove the $tRNA^{Trp}$ primer before gel electrophoresis. The cDNA products detected in virions containing the I12Lss, I12Lpk, and I4L insertions were, as expected, correspondingly larger than the wild-type $cDNA_{101}$ product (Fig. 4A and B, lanes 5, 6, and 13). The products detected in the S3L and S5L virions were the same size as those in wild-type virions (Fig. 4B, lanes 11 and 12). The amounts of strong-stop cDNA products detected in virions containing each of the loop mutations were less than those in wild-type virions. The I12L/S strong-stop cDNA product (Fig. 4A, lane 4) was undetectable, consistent with the results shown in Fig. 3A, lane 4. Surprisingly, product cDNAs derived from DS, RDS, B3DS, and B3RDS virions were below the level of detection in this assay (Fig. 4A and C, lanes 7, 8, 15, and 16), even though various but small amounts of $tRNA^{Trp}$-$dAMP_2$ products were detected in the same virions in parallel experiments when only dATP was present during synthesis (Fig. 3A). This discrepancy may result from a defect in elongation as well as initiation of reverse transcription. Purified RT has been shown to pause at duplex regions of templates, resulting in premature termination of DNA synthesis (28). Since the U5-IR extended-stem mutations are proximal to the PBS, termination at the base of the stem would result in very small cDNA products. After alkali treatment, such products would run off the gel shown in Fig. 4.

**Analysis of reverse transcription in an in vitro-reconstituted system.** To confirm that changes in the level of cDNA products synthesized in mellitin-activated mutant virions are due, in part, to defects in reverse transcription, we reconstituted similar reactions in vitro where the concentrations of RNA and enzyme are known. A series of T7 transcripts representing the 5′ untranslated region of the Rous sarcoma virus (RSV) template RNA and a $tRNA^{Trp}$ primer fragment were prepared as described in Materials and Methods. The viral RNA template represents sequences from nucleotide 1 in R to nucleotide 270 in leader. The RNA primer represents 28 nucleotides at the 3′ terminus of $tRNA^{Trp}$. The template and primer RNAs were mixed in a molar ratio of 1:5 (template to primer) and incubated with purified AMV RT under the conditions described in Materials and Methods, and the runoff cDNA products were analyzed. A DNA primer that anneals to nucleotides 20 to 40 in U5 was also added into the reaction mixture as a control for input template RNA. Both annealed primers are extended by RT in the presence of deoxynucleotides, one of which is [$\alpha$-$^{32}$P] dCTP. The sizes of the cDNA products obtained with the different viral RNA mutants primed with the tRNA fragment were the same as those detected in the corresponding mellitin-activated virions analyzed in Fig. 4. The product from the control DNA primer in all cases was 40 nucleotides and was produced in similar amounts for each reaction (Fig. 5).

The S3L (Fig. 5, lane 9) and S5L (Fig. 5, lane 8) template RNAs produced approximately threefold less $cDNA_{101}$ product than wild-type RNA (Fig. 5, lane 10), confirming that these loop substitutions decrease the efficiency of reverse transcription. A similar decrease in efficiency of reverse transcription was observed when the U5-IR loop sequences were extended by an insertion of 4 nucleotides (I4L) (Fig. 5, lane 7). The I12Lpk mutant RNA was a very poor template for in vitro reverse transcription, especially compared to I12Lss RNA. This is the case even though both mutants have a 12-nucleotide insertion in the same position in the U5-IR loop. However, this is in agreement with the results obtained in activated virions.

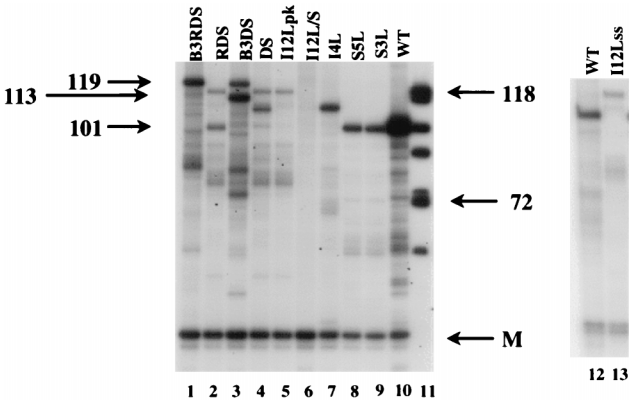


FIG. 5. Reverse transcription reconstituted in vitro requires an intact U5-IR stem and loop structure. Reverse transcription was reconstituted with a 28-mer RNA primer and wild-type (WT; lanes 10 and 12) RNA or with RNA containing U5-IR stem mutation B3RDS (lane 1), RDS (lane 2), B3DS (lane 3), or DS (lane 4), U5-IR loop mutation I12Lpk (lane 5), I4L (lane 7), S5L (lane 8), S3L (lane 9), or I12Lss (lane 13), or U5-IR stem/loop mutation I12L/S (lane 6) as described in Materials and Methods. As a control, a second long terminal repeat DNA primer was annealed to the viral RNA and yielded a cDNA extension product of 40 deoxynucleotides (M). The nucleotide length of the cDNA extension product utilizing the RNA primer for the wild type or the S5L or S3L mutant was 101; for I4L, it was 105; for RDS, DS, I12Lpk, I12L/S, or I12Lss, it was 113; and for B3RDS or B3DS, it was 119. Lane 11 contains a 5′-$^{32}$P-labeled denatured, *Hae*III-digested ϕX174 DNA marker (sizes in bases indicated).

The I12L/S insertion produced no detectable product (Fig. 5, lane 6), a result again consistent with data obtained with permeabilized virions (Fig. 3, lane 4, and Fig. 4A, lane 4). A possible explanation for the differences in the adverse effects on reverse transcription caused by these various loop mutations is presented in the Discussion.

Compared to wild-type RNA, DS and RDS RNAs each caused more than a 10-fold reduction in the amount of expected $cDNA_{113}$ extension products (Fig. 5, lanes 2 and 4). Concomitantly, significant amounts of smaller cDNA products were detected. The deleterious effect of extending the base pairing of the U5-IR stems could be partially reversed by placing 3 noncomplementary nucleotides into each strand of the RDS (Fig. 5, lane 1) or DS (Fig. 5, lane 3) stem structures. In these cases, the full-length $cDNA_{119}$ products expected from the B3DS and B3RDS mutants were obtained, but in amounts still less than the full-length wild-type product. Taken together with the data from mellitin-activated virions, these results suggest that the DS and RDS mutations cause defects in both initiation and elongation synthesis. However, the fact that introduction of the bulges in B3DS and B3RDS was not sufficient to restore elongation synthesis to detectable levels in virions (Fig. 4C, lanes 15 and 16) suggests that there is an additional defect in replication associated with these mutants.

**Measurement of viral RNA packaged into virions.** It is possible that the decrease in strong-stop cDNA or tRNA-$dAMP_2$ synthesis detected in virions could result from reduced amounts of genomic RNA packaged into virions. Although none of the previously analyzed mutations introduced into the U5 region of viral RNA caused a change in RNA packaging (12, 13), we used a primer extension strategy to quantify the levels of viral RNA encapsidated into virus particles containing each of the current U5-IR stem and loop mutations. To perform these experiments, RNA was extracted from equivalent amounts of mutant viruses and annealed to an excess of 5′-$^{32}$P-labeled DNA primer complementary to the viral RNA. In the presence of RT and four unlabeled deoxynucleotides, a runoff cDNA product is produced which is 40 deoxynucleotides. Since both the primer and RT are in excess over the template RNA and the size of the primer extension product for each mutant RNA is the same, the intensity of the radiolabeled $cDNA_{40}$ is an estimate of the amount of template RNA packaged into the particles. Moreover, since RT possesses a 5′-to-3′ RNase H activity, the RNA is degraded after one round of reverse transcription, precluding turnover during the DNA synthesis reaction. As shown in Fig. 6, primer extension analyses of RNA extracted from virus particles containing U5-IR loop mutations show that the virions contain wild-type levels of RNA. Therefore, S3L (lane 4), S5L (lane 5), and I4L (lane 6) virus mutants do not have an RNA encapsidation defect. A similar analysis of I12Lpk and I12Lss virions indicates that there are no RNA packaging defects with these mutants as well (data not shown). Thus, the defects caused by these mutations, as observed in Fig. 3 and 4, can be attributed solely to inefficient reverse transcription.

In contrast, mutant viruses with extensions of the U5-IR stem, DS (Fig. 6, lane 8), RDS (lane 10), B3DS (lane 9), and B3RDS (lane 11), all showed significant decreases in the amount of viral RNA recovered from particles. I12L/S also demonstrated an RNA encapsidation defect, as evidenced by decreased amounts of primer extension products detected in Fig. 6 (lane 7). The viruses containing the I12L/S, B3DS, and B3RDS mutations, which showed the most-delayed-growth phenotypes (Fig. 2), contained the least amounts of detectable viral RNA in their respective virions (Fig. 6). Also shown in Fig. 6 is an analysis of the amount of RNA detected in virions containing the previously described mutations S4, which disrupts the U5-IR stem, and Δ3, which deletes 3 nucleotides between the U5-IR stem and the U5-TψC interaction region. Both mutations cause defects in initiation of reverse transcription (2, 13) but, as reported, do not interfere with the packaging of viral RNA (Fig. 6, lanes 2 and 3). As a control, we analyzed the amount of RNA detected in virions containing a deletion in the leader ψ packaging signal, which causes a 10-fold decrease in packaging of viral RNA, as previously described by Katz et al. (24). This element is also sufficient to confer packaging of heterologous RNAs (5). No runoff prod-

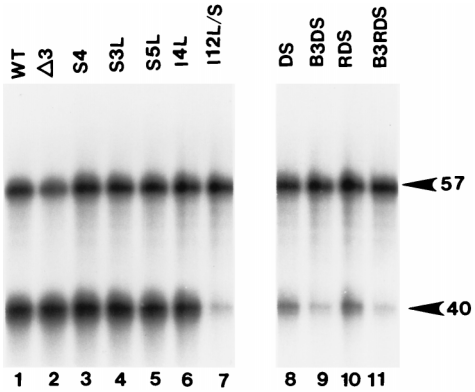


FIG. 6. Mutations to the U5-IR stem and loop affect packaging of viral RNA. The amount of RNA packaged into virions containing wild-type and mutant U5-IR stem and loop was analyzed by a primer extension assay. RNA was prepared from equivalent amounts of virus particles and annealed to excess amounts of a 20-deoxynucleotide 5′-$^{32}$P-end-labeled primer. The runoff extension reaction was carried out with unlabeled deoxynucleotides as described in Materials and Methods. The runoff product is 40 deoxynucleotides. A 5′-$^{32}$P-end-labeled 57-mer DNA was added as a recovery marker. Lane 1, wild type; lane 2, Δ3; lane 3, S4; lane 4, S3L; lane 5, S5L; lane 6, I4L; lane 7, I12L/S; lane 8, DS; lane 9, B3DS; lane 10, RDS; lane 11, B3RDS.

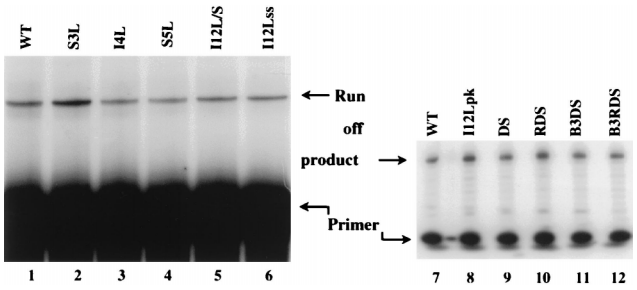


FIG. 7. Determination of the levels of viral RNA transcription in producer cell lines. Ten micrograms of total cellular RNA was analyzed by using a 5′-$^{32}$P-labeled oligodeoxynucleotide primer complementary to RSV U5 sequences in an extension assay. Shown is an autoradiogram of primer extension reactions on U5-IR mutations; the positions of the primer and its runoff product are indicated. Lanes 1 and 7, wild type; lane 2, S3L; lane 3, I4L; lane 4, S5L; lane 5, I12L/S; lane 6, I12Lss; lane 8, I12Lpk; lane 9, DS; lane 10, RDS; lane 11, B3DS; lane 12, B3RDS.

ucts from these virions were detected under our conditions (data not shown). Thus, the U5-IR stem extension mutations do not cause as strong a packaging defect as do deletions in ψ.

**Measurement of viral RNA inside the cell.** A decrease in the amount of packaged viral RNA could result from either a decreased efficiency of packaging or decreased levels of transcription inside cells. To distinguish between these two possibilities, total cellular RNA from selected cell lines expressing the different virus mutants was prepared by the guanidine thiocyanate method and equal amounts of total cellular RNA were analyzed by the same primer runoff protocol used to estimate the level of viral RNA in particles. For all of the mutations, as shown in Fig. 7, the level of viral RNA detected in cells was equal to, or greater than, the level observed with the wild type. Thus, the lack of RNA in the I12L/S, DS, RDS, B3DS, and B3RDS mutants is most likely caused by a packaging defect.

## DISCUSSION

An overall summary of the effects of the different U5-IR mutants on viral replication intermediates is presented in Table 1. Substitutions of 3 or 5 nucleotides (S3L or S5L) or insertion of 4 nucleotides (I4L) into the U5-IR loop reduces the levels of reverse transcription detected in mellitin-permeabilized virions. Considering that none of the loop mutant viruses exhibit significant RNA encapsidation defects, the DNA synthesis defects observed for S3L, S5L, and I4L (as well as the other loop mutations I12Lss and I12Lpk), can be attributed primarily to changes in reverse transcription. Since the RSV U5-IR loop is predicted to be single stranded, these results suggest that there may be a sequence-specific interaction between RT and the U5-IR loop necessary for efficient initiation of reverse transcription.

This hypothesis is further supported by comparison of the effects of the I4L and the I12Lss mutations on the initiation of reverse transcription. As summarized in Table 1, the smaller insertion mutant has a more adverse effect on reverse transcription than the larger insertion mutant. At first glance this is unexpected. However, if RT is interacting specifically with the U5-IR loop sequence, then the maintenance of a wild-type copy of the U5-IR loop sequence, AGAAG, in the same position relative to the PBS in I12Lss (see Fig. 1B), and the disruption of this sequence in I4L, suggests that I12Lss will have a less severe reverse-transcription defect than I4L. Moreover, the wild-type AGAAG sequence is also changed in S3L and S5L, which have more significant reverse-transcription initiation defects than I12Lss (Table 1). The only exception is I12Lpk, which is more defective than I12Lss, yet maintains the wild-type AGAAG loop sequence in the appropriate position. However, the I12Lpk loop sequence can base pair with complementary nucleotides located in either U5 or leader of the template RNA, thereby having the potential to form a tertiary pseudoknot. Such tertiary structures might interfere with assembly of the reverse transcription initiation complex. Alternatively, the pseudoknot structure could compete with the U5-IR loop sequences for binding to RT. It is known that HIV RT can select from a randomized population of ligands in vitro an RNA capable of forming a pseudoknot structure (45). In addition, there is some evidence that the equivalent loop sequences in duck hepatitis B virus are important for initiation of reverse transcription. In this case, reverse transcription is reduced when recognition of the loop region by the P protein is altered (44).

Although the experimental evidence described above suggests that the U5-IR loop is involved in initiation of reverse transcription, this does not preclude the loop sequence from playing a role in elongation, as has been reported by Isel et al. for HIV-1 RNA (21). This might explain some of the subtle differences seen between synthesis of loop mutant $tRNA^{Trp}$-$dAMP_2$ and strong-stop cDNA products observed in mellitin-activated virions (Table 1).

Extensions of the duplex structure of the U5-IR stem (DS, which inserts 12 nucleotides and duplicates in tandem most of the stem structure, or RDS, which introduces a random sequence into the stem) show larger decreases in reverse transcription than U5-IR loop mutations. This is due most likely to the stem extensions causing decreases in the efficiency of elongation as well as in initiation of reverse transcription. RT has difficulty using hairpin structures as templates. This hypothesis is supported by the B3DS and B3RDS mutations, which reduce the contiguous length of the extended U5-IR stem duplexes and result in increased reverse transcription (compared to DS and RS) observed in vitro. Since the DS and the RDS muta-

TABLE 1. Summary of effects of U5-IR mutations on viral replication intermediates[a]

| Mutant[b] | $tRNA^{Trp}$-[dA][c] | Strong-stop cDNA[d] | In vitro reverse transcription[e] | RNA packaging in virions[f] |
|---|---|---|---|---|
| Wild type | +++++ | +++++ | +++++ | +++++ |
| S3L | Not done | ++ | ++ | +++++ |
| S5L | +++++ | ++ | ++ | +++++ |
| I4L | +++ | ++ | ++ | +++++ |
| I12Lss | +++++ | ++++ | ++++ | +++++ |
| I12Lpk | +++ | + | + | +++++ |
| I12L/S | ND | ND | ND | + |
| DS | + | ND | + | ++ |
| RDS | + | ND | + | ++ |
| B3DS | ++ | ND | ++ | + |
| B3RDS | ++ | ND | ++ | + |

[a] The values in this table have been corrected for internal controls. All the values are defined relative to the wild type. ND, <1%; +, 1 to 20%; ++, 21 to 40%; +++, 41 to 60%; ++++, 61 to 80%; +++++, 81 to 100%.

[b] U5-IR mutants are defined in Results and depicted in Fig. 1B.

[c] Amount of $tRNA^{Trp}$-[dA] product formed in mellitin-activated virions, as presented in Fig. 3.

[d] Amount of minus-strand strong-stop cDNA produced in mellitin-activated virions, as presented in Fig. 4.

[e] Amount of minus-strand strong-stop cDNA produced in reconstituted reverse transcription reactions, as presented in Fig. 5.

[f] Amount of genomic RNA encapsidated in virions, as presented in Fig. 6.

tions both possess wild-type U5-IR loop sequences, the observed adverse effects on reverse transcription must be caused by the changes placed into the stem structures.

None of the mutations analyzed in this report are predicted to affect integration. To confirm this, in vitro integration assays were performed on preprocessed oligodeoxynucleotides representing wild-type and selected mutant sequences (S3L, S5L, I4L, and I12L/S). While this assay system does not exhibit the concerted properties associated with integration in vivo (4, 5), failure to catalyze the joining reaction in vitro would indicate that there could be an integration defect in vivo. DNA containing the S3L, S5L, I4L, or I12L mutation did not appear to be defective in integration (data not shown). DNAs representing integration protein recognition sites containing the DS, RDS, B3DS, and B3RDS mutations were not tested. However, these mutations change the same deoxynucleotides affected by the above model DNA substrates and are therefore predicted to have no effect on integration.

Sequences found in the U5-IR stem and loop are highly conserved among avian retrovirus RNAs. They also bear a striking similarity to other sequences in the leader, which are required for encapsidation of RSV RNA into virions (5, 24). This sequence homology is as follows, where the underlined sequence defines the inverted repeat that forms the U5-IR stem.

$_{217}$U*G***C***GG***CU**U*AGGAGGG***C***AGAAG*CUGA$_{241}$ leader RNA (ψ)
$_{73}$A*G***C***AC***CU**G*AAUGAAG***C***AGAAG*GCUUCAU$_{100}$ U5-IR stem

The bold letters highlight the sequence identity, and the italicized letters highlight aligned purines. This homology is one of the observations that prompted us to examine the RNA content in virions containing the altered U5-IR stem-loop structures, despite that fact that the previously studied mutant, S4, which disrupts the stem, perturbed initiation of reverse transcription without affecting packaging (12). Like S4, the U5-IR loop substitutions, S3L and S5L, and the loop insertions, I4L, I12Lss, and I12Lpk, had little detectable effect on the amount of viral RNA packaged into virions (see Table 1). Thus, neither the integrity of the U5-IR stem-loop nor the direct homology between the U5-IR loop sequence and the RSV leader ψ packaging signal is necessary for efficient encapsidation of viral RNA into virions. However, primer extension analyses of the I12L/S, DS, RDS, B3DS, and B3RDS mutants detected significant decreases in the levels of RNA packaged into virions. At the same time, viral RNA transcription was found to be normal in infected cells, suggesting that the U5-IR stem region plays a role in RNA packaging. From the nature of the mutations analyzed, particularly DS and RDS, we suggest that this role is not sequence specific. It is possible that the U5-IR stem extensions may interfere with formation of a wild-type structure necessary for efficient RNA packaging involving the leader ψ sequence.

One common feature observed in all RNA sequences implicated in packaging, including the U5-IR stem, is the presence of stem-loop structures. This is true for bovine leukemia virus (33), spleen necrosis virus (48), Mo-MuLV (36, 39), RSV (5, 24), and HIV-1 (10, 11, 18, 30, 34, 49). Packaging signals also appear to involve multiple RNA components. In HIV-1, the sequences necessary for RNA encapsidation span the 5′ splice site in the leader and consist of four stem-loop structures (11, 19, 30, 34). This region is sufficient in itself to direct the specific packaging of viral RNA (19). In Mo-MuLV, the ψ sequence is sufficient to confer packaging on heterologous nonviral RNAs. However, the titers of the resultant viruses vary depending upon the specific location of the packaging signal in the proviral vector (32). Additionally, deletions in the 5′ half of the U5 region of Mo-MuLV also decrease RNA packaging to the same extent as the ψ mutant (39). Murphy and Goff suggested that it may not be the sequences themselves or the structures that they form but rather the overall topology of the RNA molecule that directs efficient packaging. The finding that disruption of the RSV U5-IR stem by the S4 mutation does not cause a packaging defect while the nucleotide extensions of the stem do, seems to support this idea.

The avian sarcoma-leukosis virus U5 and leader regions are not only highly structured but also contain several small open reading frames (ORFs) upstream of the *gag* translation start codon (17). Several laboratories have suggested that perturbation of one or more of these ORFs leads to an RNA encapsidation defect due to interference with the normal balance between RNA packaging and protein translation (15, 16, 26, 38, 40). Specifically, decreased encapsidation was reported when mutations were introduced which affected translation efficiency of the 1st and 3rd ORF downstream from the 5′ end of the viral RNA. Mutations decreasing the size of the 2nd ORF also caused packaging defects, but in conjunction with reductions in translation initiation at the 3rd ORF. In contrast, mutations extending the size of the 2nd ORF, with or without secondary structure, did not affect packaging detectably (15, 16). The insertions into the U5-IR stem and loop studied in this report are within the 2nd ORF. Since they are insertions that would increase the size of the ORF, it is likely that the observed deficiency in RNA encapsidation is not due to changes in translation or ribosome scanning.

In vivo, the 5′ untranslated RSV RNA is involved in several processes in replication, including reverse transcription, protein translation, packaging of viral RNA, and, at the level of DNA, integration. These processes occur at different times during the replication cycle. Therefore, there must be balance between the multiple functions of these RNA sequences in order to ensure successful replication. This balance may be achieved in part by the presence of specific structural and sequence elements in this region of RNA that dictate which proteins form functional complexes at different times.

## ACKNOWLEDGMENTS

J.T.M. and Z.G. contributed equally to this work.

This work was supported in part by Public Health Service grant CA38046 from the National Cancer Institute. J.T.M. was supported in part by funds from AIDS Institutional Training grant AI07381 from the National Institutes of Health. S.M. is a Medical Scientist Trainee supported by grant GM07250 from the National Institutes of Health.

We especially thank Richard Katz, Fox Chase Cancer Center, for the leader ψ minus deletion mutant.

## REFERENCES

1. **Aiyar, A., D. Cobrinik, Z. Ge, H.-J. Kung, and J. Leis.** 1992. Interaction between retroviral U5 RNA and the TψC loop of the tRNA$^{Trp}$ primer is required for efficient initiation of reverse transcription. J. Virol. **66:**2464–2472.
2. **Aiyar, A., Z. Ge, and J. Leis.** 1994. A specific orientation of RNA secondary structures is required for initiation of reverse transcription. J. Virol. **68:**611–618.
3. **Aiyar, A., Y. Xiang, and J. Leis.** 1995. Site-directed mutagenesis using overlap extension PCR. Methods Mol. Biol. **57:**177–191.
4. **Aiyar, A., P. Hindmarsh, A. M. Skalka, and J. Leis.** 1996. Concerted integration of linear retroviral DNA by the ASV integrase in vitro: dependence on both long terminal repeat termini. J. Virol. **70:**3571–3580.
5. **Aronoff, R., A. M. Hajjar, and M. Linial.** 1993. Avian retroviral RNA encapsidation: reexamination of functional 5′ RNA sequences and the role of nucleocapsid Cys-His motifs. J. Virol. **67:**178–188.
6. **Arts, E., M. Ghosh, P. Jacques, B. Ehresmann, and S. LeGrice.** 1996. Restoration of tRNA-primed minus strand DNA synthesis to a reverse transcriptase mutant with tRNA/DNA chimeras: tRNA-viral RNA duplexes and initiation of HIV replication. J. Biol. Chem. **271:**9054–9061.

7. **Arts, E., S. Stetor, X. Li, J. Rausch, K. Howard, B. Ehresmann, T. North, B. Wohrl, R. Goody, M. Wainberg, and S. LeGrice.** 1996. Initiation of minus strand DNA synthesis from $tRNA^{Lys,3}$ on lentiviral RNAs: implications of specific HIV-1 RNA-$tRNA^{Lys,3}$ interactions inhibiting primer utilization by retroviral reverse transcriptases. Proc. Natl. Acad. Sci. USA **93:**10063–10068.
8. **Baudin, F., R. Marquet, C. Isel, J.-L. Darlix, B. Ehresmann, and C. Ehresmann.** 1993. Functional sites in the 5′ region of HIV-1 RNA form defined structural domains. J. Mol. Biol. **229:**382–397.
9. **Berkhout, B., and I. Schoneveld.** 1993. Secondary structure of HIV-2 leader RNA comprising the tRNA-primer binding site. Nucleic Acids Res. **21:**1171–1178.
10. **Clavel, F., and J. Orenstein.** 1990. A mutant of human immunodeficiency virus with reduced RNA packaging and abnormal particle morphology. J. Virol. **64:**5230–5234.
11. **Clever, J., C. Saddetti, and T. Parslow.** 1995. RNA secondary structure and binding sites for *gag* gene products in the 5′ packaging signal of human immunodeficiency virus type 1. J. Virol. **69:**2101–2109.
12. **Cobrinik, D., A. Aiyar, Z. Ge, M. Katzman, H. Huang, and J. Leis.** 1991. Overlapping retroviral U5 sequence elements are required for efficient integration and initiation of reverse transcription. J. Virol. **65:**3864–3872.
13. **Cobrinik, D., L. Soskey, and J. Leis.** 1988. A retroviral RNA secondary structure required for efficient initiation of reverse transcription. J. Virol. **62:**3622–3630.
14. **Cordell, B., R. Swanstrom, H. M. Goodman, and J. M. Bishop.** 1979. $tRNA^{Trp}$ as primer for RNA-directed DNA polymerase: structural determinants of function. J. Biol. Chem. **254:**1866–1874.
15. **Donze, O., and P.-F. Spahr.** 1992. Role of the open reading frames of Rous sarcoma virus leader RNA in translation and genome packaging. EMBO J. **11:**3747–3757.
16. **Donze, O., P. Damay, and P.-F. Spahr.** 1995. The first and third uORFs in RSV leader RNA are efficiently translated: implications for translational regulation and viral RNA packaging. Nucleic Acids Res. **23:**861–868.
17. **Hackett, P. B., M. W. Dalton, D. P. Johnson, and R. B. Petersen.** 1991. Phylogenetic and physical analysis of the 5′ leader RNA sequences of avian retroviruses. Nucleic Acids Res. **19:**6929–6934.
18. **Harrison, G., and A. Lever.** 1992. The human immunodeficiency virus type 1 packaging signal and major splice donor region have a conserved stable secondary structure. J. Virol. **66:**4144–4153.
19. **Hayashi, T., T. Shioda, Y. Iwakura, and H. Shibuta.** 1992. RNA packaging signal of human immunodeficiency virus type 1. Virology **188:**590–599.
20. **Isel, C., C. Ehresmann, G. Keith, B. Ehresmann, and R. Marquet.** 1995. Initiation of reverse transcription of HIV-1: secondary structure of the HIV-1 RNA/$tRNA^{Lys,3}$ template/primer. J. Mol. Biol. **247:**236–250.
21. **Isel, C., J.-M. Lanchy, S. LeGrice, C. Ehresmann, B. Ehresmann, and R. Marquet.** 1996. Specific initiation and switch to elongation of human immunodeficiency virus type 1 reverse transcription require the post-transcriptional modifications of primer $tRNA^{Lys,3}$. EMBO J. **15:**917–924.
22. **Kang, S.-M., J. Wakefield, and C. Morrow.** 1996. Mutations in both the U5 region and primer binding site influence the selection of the tRNA used for initiation of HIV-1 reverse transcription. Virology **222:**401–414.
23. **Kang, S.-M., Z. Zhang, and C. Morrow.** 1997. Identification of a sequence within U5 required for human immunodeficiency virus type 1 to stably maintain a primer binding site complementary to $tRNA^{Met}$. J. Virol. **71:**207–217.
24. **Katz, R., R. Terry, and A. M. Skalka.** 1986. A conserved *cis*-acting sequence in the 5′ leader of avian sarcoma virus RNA is required for packaging. J. Virol. **59:**163–167.
25. **Katzman, M., R. A. Katz, A. M. Skalka, and J. Leis.** 1989. The avian retroviral integration protein cleaves the terminal sequences of linear viral DNA at the in vivo sites of integration. J. Virol. **63:**5319–5327.
26. **Knight, J. B., Z. H. Si, and C. M. Stoltzfus.** 1994. A base-paired structure in the avian sarcoma virus 5′ leader is required for efficient encapsidation of RNA. J. Virol. **68:**4493–4502.
27. **Kohlstaedt, L. A., and T. A. Steitz.** 1992. Reverse transcriptase of human immunodeficiency virus can use either human $tRNA^{Lys,3}$ or *Escherichia coli* $tRNA^{Gln,2}$ as primer in an *in vitro* primer-utilization assay. Proc. Natl. Acad. Sci. USA **89:**9652–9656.
28. **Leis, J.** 1976. RNA-dependent DNA polymerase activity of RNA tumor viruses. J. Virol. **19:**932–939.
29. **Leis, J., A. Aiyar, and D. Cobrinik.** 1993. Regulation of initiation of reverse transcription of retroviruses, p. 33–47. *In* A. M. Skalka and S. P. Goff (ed.), Reverse transcriptase. Cold Spring Harbor Laboratory Press, Cold Spring Harbor, N.Y.
30. **Lever, A., H. Gottlinger, W. Haseltine, and J. Sodroski.** 1989. Identification of a sequence for efficient packaging of human immunodeficiency virus type 1 RNA into virions. J. Virol. **63:**4085–4087.
31. **Li, X., J. Mak, E. J. Arts, Z. Gu, L. Kleiman, M. A. Wainberg, and M. A. Parniak.** 1994. Effects of alterations of primer-binding site sequences on human immunodeficiency virus type 1 replication. J. Virol. **68:**6198–6206.
32. **Mann, R., and D. Baltimore.** 1985. Varying the position of a retrovirus packaging sequence results in the encapsidation of both unspliced and spliced RNAs. J. Virol. **54:**401–407.
33. **Mansky, L. M., A. E. Krueger, and H. M. Temin.** 1995. The bovine leukemia virus encapsidation signal is discontinuous and extends into the 5′ end of the *gag* gene. J. Virol. **69:**3282–3289.
34. **McBride, S., and A. Panganiban.** 1996. The human immunodeficiency virus type 1 encapsidation site is a multipartite RNA element composed of functional hairpin structures. J. Virol. **70:**2963–2973.
35. **Milligan, J., D. Groebe, G. Witherell, and O. Uhlenbeck.** 1987. Oligoribonucleotide synthesis using T7 RNA polymerase and synthetic DNA templates. Nucleic Acids Res. **15:**8783–8798.

35a. **Morris, S., and J. Leis.** Unpublished data.

36. **Mougel, M., Y. Zhang, and E. Barklis.** 1996. *cis*-active structural motifs in specific encapsidation of Moloney murine leukemia virus RNA. J. Virol. **70:**5043–5050.
37. **Mougel, M., N. Touneki, J.-L. Darlix, J. Paoletti, B. Ehresmann, and C. Ehresmann.** 1993. Conformational analysis of the 5′ leader and the gag initiation site of Mo-MuLV RNA and allosteric transitions induced by dimerization. Nucleic Acids Res. **21:**4677–4684.
38. **Moustakas, A., T. Sonstegaard, and P. Hackett.** 1993. Alterations of the three short open reading frames in the Rous sarcoma virus leader RNA modulate viral replication and gene expression. J. Virol. **67:**4337–4349.
39. **Murphy, J. E., and S. P. Goff.** 1989. Construction and analysis of deletion mutations in the U5 region of Moloney murine leukemia virus: effects on RNA packaging and reverse transcription. J. Virol. **63:**319–327.
40. **Parkin, N. T., E. A. Cohen, A. Darveau, C. Rosen, W. Haseltine, and N. Sonenberg.** 1988. Mutational analysis of the 5′ non-coding region of human immunodeficiency virus type 1: effects of secondary structure on translation. EMBO J. **7:**2831–2837.
41. **Rizvi, T., and A. Panganiban.** 1993. Simian immunodeficiency virus RNA is efficiently encapsidated by human immunodeficiency virus type 1 particles. J. Virol. **67:**2681–2688.
42. **Sambrook, J., E. F. Fritsch, and T. Maniatis.** 1989. Molecular cloning: a laboratory manual, 2nd ed. Cold Spring Harbor Laboratory Press, Cold Spring Harbor, N.Y.
43. **Schwartz, D. E., R. Tizard, and W. Gilbert.** 1983. Nucleotide sequence of Rous sarcoma virus. Cell **22:**853–869.
44. **Tavis, J. E., and D. Ganem.** 1995. RNA sequences controlling the initiation and transfer of duck hepatitis B virus minus-strand DNA. J. Virol. **69:**4283–4291.
45. **Tuerk, C., S. MacDougal, and L. Gold.** 1992. RNA pseudoknots that inhibit human immunodeficiency virus type 1 reverse transcriptase. Proc. Natl. Acad. Sci. USA **89:**6988–6992.
46. **Wakefield, J. K., and C. D. Morrow.** 1996. Mutations within the primer binding site of human immunodeficiency virus type 1 define sequence requirements essential for reverse transcription. Virology **220:**290–298.
47. **Wakefield, J. K., S. M. Kang, and C. D. Morrow.** 1996. Construction of a type 1 human immunodeficiency virus that maintains a primer binding site complementary to $tRNA^{His}$. J. Virol. **70:**966–975.
48. **Yang, S., and H. Temin.** 1994. A double hairpin structure is necessary for the efficient encapsidation of spleen necrosis virus retroviral RNA. EMBO J. **13:**713–726.
49. **Zhang, Y., and E. Barklis.** 1995. Nucleocapsid protein effects on the specificity of retrovirus RNA encapsidation. J. Virol. **69:**5716–5722.
50. **Zhang, Z., S.-M. Kang, A. LeBlanc, S. Hajduk, and C. Morrow.** 1996. Nucleotide sequences within the U5 region of the viral RNA genome are the major determinants for an human immunodeficiency virus type 1 to maintain a primer binding site complementary to $tRNA^{His}$. Virology **226:**306–317.